J. Phys. B: At. Mol. Opt. Phys. **25** (1992) 61-70. Printed in the UK

Analysis of the projection of the total orbital angular momentum along the interelectronic axis for doubly excited states of atoms

Z Chen†, C-G Bao‡ and C D Lin†

† Department of Physics, Kansas State University, Manhattan, KS, USA
‡ Department of Physics, Zhong-Shan University, Guangzhou, People's Republic of China
and
CCAST (World Laboratory), PO Box 8730, Beijing 100080, People's Republic of China

Received 21 May 1991

Abstract. Doubly excited states of two-electron atoms and ions are calculated using the configuration interaction method and the resulting wavefunctions are analysed in the body frame of the atom. We computed the percentage of the projection (T) of the total orbital angular momentum L along the interelectronic axis for the $3l3l'$ and $3l4l'$ doubly excited states. It is shown that along each rotor series, the projection is dominated by a single T component for small-L states and that these states are well described by the molecular model. For the high-L states along the rotor series, admixture of different T components is large and these states display properties characteristic of a shell model. The relation between the purity of T projection and the T doubling is also discussed.

1. Introduction

The existence of molecule-like normal modes of a pair of electrons in doubly excited states of atoms has been established in the last two decades from a number of different theoretical viewpoints (Herrick 1983, Berry 1989, Lin 1986 and references therein). Typical 'molecular behaviour' such as the rotor structure and the Λ-doubling have been observed in the calculated energy levels of doubly excited states (Kellman and Herrick 1980, Lin 1984). Further evidence of the 'molecular behaviour' has been provided by displaying the wavefunctions (or equivalently the electronic densities) in the conventional independent particle coordinates (Ezra and Berry 1983) or in hyperspherical coordinates (Lin 1982, 1984). Two molecular approaches have been introduced to study such doubly excited states of atoms. One is based on treating the two-electron atom as a linear ABA triatomic molecule (see Berry 1989 and references therein) where A represents the electron and B the nucleus. The other is to treat the doubly excited states of atoms like the H_2^+ molecule where the role of the electron and the heavy particle is reversed (Feagin and Briggs 1987, 1988, Rost and Briggs 1988). It has been shown that the energy levels, the radiative and Auger decay rates of doubly excited states can be interpreted qualitatively using either molecular model (Atsumi *et al* 1991, Chen and Lin 1989, Gou *et al* 1991, Hunter and Berry 1987, Vollweiter *et al* 1991).

In the conventional approach, doubly excited states of atoms can be calculated using the configuration interaction (CI) method. For these states the mixing of different configurations is quite large such that the designation based on the independent particle model is inadequate. For intrashell doubly excited states, it has been shown that the

0953-4075/92/010061+10$04.50

wavefunctions can be approximated by the eigenfunctions which diagonalize the operators $\boldsymbol{B}^2=(\boldsymbol{b}_1-\boldsymbol{b}_2)^2$ and $(\boldsymbol{L}\cdot\boldsymbol{B})^2$ (Wulfman 1973, Herrick and Sinanoglu 1975), see equations (1) and (2) below. These eigenfunctions, labelled by the new K and T quantum numbers, are called doubly excited states basis (DESB) functions. The K and T, which are exact quantum numbers of the DESB functions, can then serve as the approximate quantum numbers of doubly excited states, replacing the l_1 and l_2 quantum numbers used in the independent electron model.

The K and T quantum numbers were adopted and extended later by Lin (1983, 1984) where each doubly excited state is designated by ${}_n(K,T)^A_N$ in addition to the usual L, S and π quantum numbers. This notation preserves the approximate quantum numbers used in the independent electron model, such as n and N, which are the principal quantum numbers of the outer and the inner electrons, respectively. The superscript A, which is *not* an independent quantum number, was introduced to emphasize the nature of the radial motion of the two electrons with respect to the nucleus. Further details about this classification scheme can be found in the review by Lin (1986).

The relation between the different classification schemes has been discussed in the literature (Feagin and Briggs 1988, Chen and Lin 1990). By treating each set of quantum numbers as approximate, there is a one-to-one correspondence between the (K, T) quantum numbers and those used in the molecular approaches. On the other hand, it is important to assess the deviation and the limitation of the molecular description. One of the major features of the molecular description is that the projection of the total orbital angular momentum along one of the principal axes in the body frame is a good quantum number. Thus, a similar projection can be used to measure the molecular character of each doubly excited state of atoms.

The group-theoretical work of Herrick and co-workers has shown that the quantum number T in the DESB functions can be interpreted approximately as the projection of the total L along the interelectronic axis. Recall that T is the eigenvalue of $(\boldsymbol{L}\cdot\boldsymbol{B})^2$. According to O(4), the expectation value of the Lenz vector $\boldsymbol{b}$ is proportional to the expectation value of $\boldsymbol{r}$,

$$\langle \boldsymbol{r}\rangle=\frac{3n}{2Z}\langle \boldsymbol{b}\rangle \tag{1}$$

where n is the principal quantum number. This relation allows one to write (Watanabe and Lin 1986)

$$\boldsymbol{B}=\frac{2}{3}\left[\frac{Z_1}{n_1}\boldsymbol{r}_{12}+\left(\frac{Z_1}{n_1}-\frac{Z_2}{n_2}\right)\boldsymbol{r}_2\right] \tag{2}$$

where Z_1 and Z_2 are the effective charges of the outer and the inner electrons, respectively. In the limit of intrashell states where $n_1=n_2=n$ and $Z_1=Z_2=Z$, $\boldsymbol{B}$ is proportional to $\boldsymbol{r}_{12}$ and thus T is the projection of the orbital angular momentum along the interelectronic axis. In the limit that $r_1\gg r_2$, $\boldsymbol{B}$ is again proportional to $\boldsymbol{r}_{12}$ if one neglects terms of order n_2/n_1. Thus the T quantum number can be interpreted as the projection of L along the interelectronic axis. In this connection, T is identical to the Λ quantum number of a diatomic molecule. For a given total orbital angular momentum L of an atom, T ranges from $0, 1, 2, \ldots, L$. Since T is only an approximate quantum number for each doubly excited state, in this article we adopt the definition that the 'molecular character' of each state is measured by the purity of the T-projection of that state along the interelectronic axis.

In order to assess the purity of T-projection for a large number of states and its connection with the rovibrational characters of doubly excited states, we use the configuration interaction method to obtain the two-electron wavefunctions. This is in contrast to the earlier study of Watanabe and Lin (1986) where the T-projection was investigated at a number of fixed values of hyperradius R using wavefunctions calculated in hyperspherical coordinates. The computation and the method of analysis are described in section 2. The results are discussed in section 3 and a short summary in section 4.

The validity of the molecular model of atoms has been studied by Hunter and Berry (1987) also where they calculated the overlap of the CI wavefunctions and the rotor–vibrator wavefunctions for doubly excited states of He and alkaline-earth atoms. Only the low-lying states were examined. The present calculation covers a larger number of states, but only the T-projection is investigated.

2. Theoretical method of analysis

The non-relativistic Hamiltonian for the two-electron system considered is

$$H = -\tfrac{1}{2}\nabla_1^2 - \tfrac{1}{2}\nabla_2^2 - Z/r_1 - Z/r_2 + 1/r_{12} = H_1 + H_2 + 1/r_{12}. \tag{3}$$

In the CI calculation the basis functions are constructed from the (anti)symmetrized product of hydrogenic wavefunctions,

$$\begin{aligned}\Phi^{LMS}_{n_1 l_1 n_2 l_2}(\boldsymbol{r}_1, \boldsymbol{r}_2) &= \sqrt{\tfrac{1}{2}}(R_{n_1 l_1}(r_1) R_{n_2 l_2}(r_2)\, Y_{l_1 l_2 LM}(\hat{\boldsymbol{r}}_1, \hat{\boldsymbol{r}}_2) \\ &\quad + (-1)^S R_{n_1 l_1}(r_2) R_{n_2 l_2}(r_1)\, Y_{l_1 l_2 LM}(\hat{\boldsymbol{r}}_2, \hat{\boldsymbol{r}}_1))\end{aligned} \tag{4}$$

where Y is the two-particle coupled orbital angular momentum function and $R_{nl}(r)$ is the radial solution of the single particle Hamiltonian. Doubly excited states are usually embedded in the continuum. We obtain the 'bound state' part by excluding orbitals in the basis functions which have lower principal quantum numbers than the states of interest. The CI wavefunction is then given by

$$\Psi_i^{LMS}(\boldsymbol{r}_1, \boldsymbol{r}_2) = \sum_{n_1 l_1 n_2 l_2} a^i_{n_1 l_1 n_2 l_2} \Phi^{LMS}_{n_1 l_1 n_2 l_2}(\boldsymbol{r}_1, \boldsymbol{r}_2). \tag{5}$$

In the present calculation, a relatively large CI basis set was used. For the $3l3l'$ and $3l4l'$ doubly excited states studied the number of basis functions is about 80–100. The values of n_1 were fixed to 3 and 4, with $0 < l_1 < n_1$. The values of n_2 range from 3 to 8, with the range of l_2 determined by the total L, S and π. The wavefunctions calculated from such a basis set are then analysed.

In the body frame the wavefunction takes the form

$$\Psi_i^{LMS}(\boldsymbol{r}_1, \boldsymbol{r}_2) = \sum_{Q=-L}^{L} \psi^i_{LQ}(r_1, r_2, \theta_{12}) D^L_{QM}(\alpha, \beta, \gamma) \tag{6}$$

where $D^L_{QM}(\alpha, \beta, \gamma)$ is the rotation matrix and $\psi^i_{LQ}(r_1, r_2, \theta_{12})$ is only a function of the radii of the two electrons and the angle between them measured from the nucleus. We choose the body-frame z axis to be along the interelectronic axis and the x axis on the plane spanned by $\boldsymbol{r}_1$ and $\boldsymbol{r}_2$. Under such a rotation, the radial part of the wavefunctions remains the same, but the angular part becomes

$$Y^{LM}_{l_1 l_2}(\hat{\boldsymbol{r}}_1, \hat{\boldsymbol{r}}_2) = \sum_Q Y_{l_1 l_2 LQ}(\theta_1', 0; \theta_2', 0) D^L_{QM}(\alpha, \beta, \gamma) \tag{7}$$

where θ_1' and θ_2' are angles of the two electrons with respect to the z axis in the body frame. From the geometry it is clear that

$$\cos\theta_1' = \frac{r_1 - r_2\cos\theta_{12}}{(r_1^2 + r_2^2 - 2r_1r_2\cos\theta_{12})^{1/2}} \tag{8a}$$

$$\cos\theta_2' = -\frac{r_2 - r_1\cos\theta_{12}}{(r_1^2 + r_2^2 - 2r_1r_2\cos\theta_{12})^{1/2}}. \tag{8b}$$

We can rewrite (6) in terms of symmetrized D functions as

$$\Psi_i^{LMS}(r_1, r_2) = \sum_{T=0}^{L} \psi_{LT}^i(r_1, r_2, \theta_{12}) \times\sqrt{\tfrac{1}{2}}\, N(D_{TM}^L(\alpha,\beta,\gamma) + \pi(-1)^{L+T}D_{-TM}^L(\alpha,\beta,\gamma)) \tag{9}$$

where $N = 1$ if $T \neq 0$ and $N = 1/\sqrt{2}$ if $T = 0$, and

$$\psi_{LT}^i(r_1, r_2, \theta_{12}) = \sum_{n_1 l_1 n_2 l_2} a_{n_1 l_1 n_2 l_2}^i \sqrt{\tfrac{1}{2}}(R_{n_1 l_1}(r_1)R_{n_2 l_2}(r_2)Y_{l_1 l_2 LT}(\theta_1', 0; \theta_2', 0) + (-1)^S R_{n_1 l_1}(r_2)R_{n_2 l_2}(r_1)Y_{l_1 l_2 LT}(\theta_2', 0; \theta_1', 0)). \tag{10}$$

The integration of $|\psi_{LT}|^2$ over r_1, r_2 and θ_{12} gives the fraction of the projection of the total angular momentum along the interelectronic axis with component T. The three-dimensional integration can be carried out using Gauss-Laguerre and Gauss-Legendre quadratures.

3. Results and discussion

3.1. The purity of the T-projection along the ${}_3(2, 0)_3^+$ rotor series

Doubly excited states which have identical K and T quantum numbers are known to form a truncated rotor series. In figure 1, we examine the purity of the $T = 0$ component

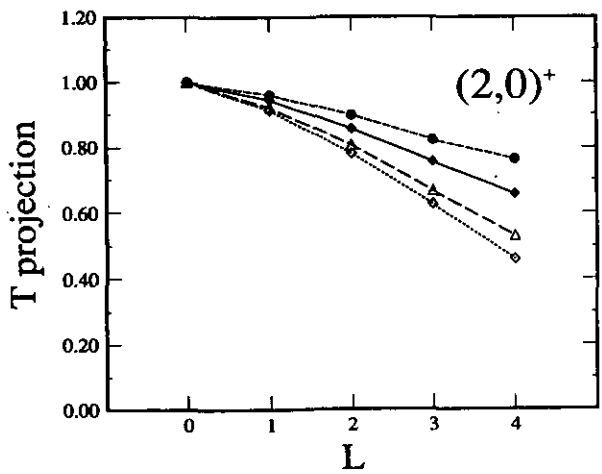

Figure 1. Fraction of the $T = 0$ component of the projection of L along the interelectronic axis for the ${}_3(2, 0)_3^+$ rotor series of H^- (full circles), He (full diamonds), C^{4+} (triangles) and DESB functions (open diamonds).

along the ${}_3(2,0)_3^+$ rotor series for different systems. This rotor series is truncated at ${}^1G^e$, i.e. $L=4$. Four systems are included, H^- (full circles), He (full diamonds), C^{4+} (triangles) and DESB states (open diamonds). The DESB states are the eigenstates for the system where the nuclear charge approaches infinity. For the ${}^1S^e$ state, the total L is zero and the projection has 100% $T=0$ component. As L increases, the fraction of $T=0$ component decreases. Recall that in the molecular interpretation, T is an exact quantum number. Thus the purity of T reflects the accuracy of the molecular representation. In this respect, the ${}_3(2,0)_3^+$ rotor series of H^- is more 'molecular' than He, which in turn is more 'molecular' than C^{4+}. The DESB functions, which are the eigenstates corresponding to $Z\to\infty$, are the least 'molecular'. For the last member of this rotor series, ${}^1G^e$, it has 52% of the $T=0$ component for C^{4+}. This fraction increases to 65% for He and to 80% for H^-. From the CI viewpoint, this increasing purity is related to stronger intershell mixing as Z decreases, as well as to the gradual decrease of the shell structure.

The truncation of the rotor series, which is not predicted by the molecular models, is related to the failure of the later models for describing the high-L members of the rotor series. These high-L members still preserve a number of aspects of the shell model of atoms. Thus these states show rotational contraction with increasing L (which can be easily interpreted using the shell model (Dunn *et al* 1990)) rather than the rotational expansion expected from the molecular model.

3.2. The purity of the T-projection along the ${}_3(1,1)_3^+$ and ${}_4(2,0)_3^-$ rotor series

In figure 2 we show the T-projection for the ${}_3(1,1)_3^+$ rotor series of He and for DESB states. This rotor series has three states, ${}^1P^o$, ${}^3D^e$ and ${}^1F^o$, with $T=1$ as the dominant component and the series terminates at $L=3$. The lowest state again has a large fraction of the $T=1$ component and may be viewed as 'molecular' in that the projection of L along the interelectronic axis is almost a good quantum number. For the $L=3$ state, the $T=0$ component is about as large as the $T=1$ component, and this state is not well represented by a molecular picture.

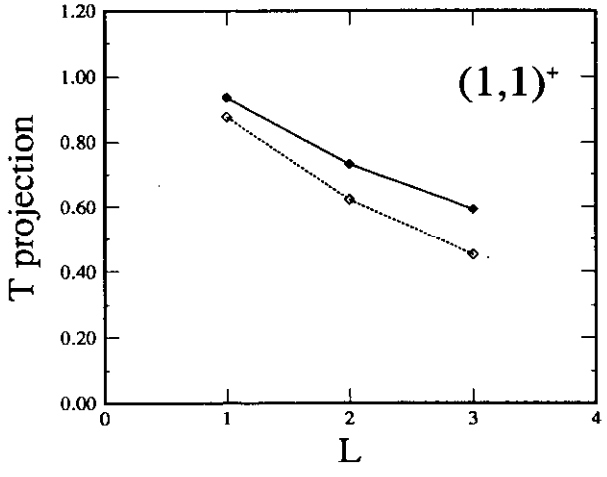

Figure 2. Fraction of the $T=1$ component of the projection of L along the interelectronic axis for the ${}_3(1,1)_3^+$ rotor series of He (full diamonds) and DESB functions (open diamonds).

In figure 3 we show the fraction of the $T = 0$ component for the ${}_4(2, 0)_3^-$ rotor series for He and for DESB functions. This group belongs to the manifold of $3l4l'$ doubly excited states. The purity of the $T = 0$ component for this series is less than that for the ${}_3(2, 0)_3^+$ rotor series considered in figure 1, but the difference is small.

3.3. The purity of T-projection along the double Rydberg series

We expect doubly excited states to become more 'molecular' as the principal quantum numbers of the doubly excited states increase. In figure 4 we compare the purity of

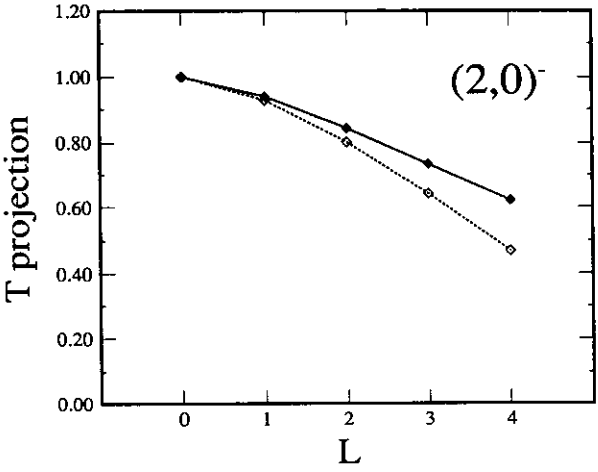

Figure 3. Fraction of the $T = 0$ component of the projection of L along the interelectronic axis for the ${}_4(2, 0)_3^-$ rotor series of He (full diamonds) and DESB functions (open diamonds).

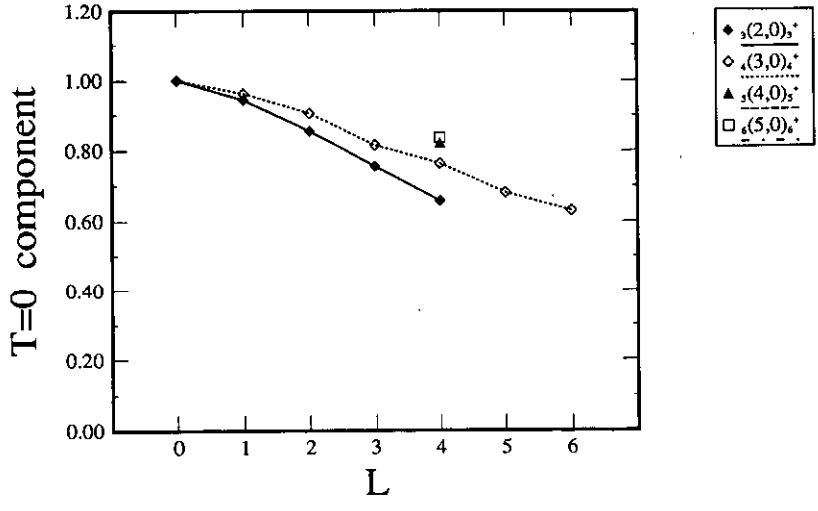

Figure 4. Fraction of the $T = 0$ component of the projection of L along the interelectronic axis for the ${}_N(N-1, 0)_N^+$ double Rydberg series of He. $N = 3$, full diamonds; $N = 4$, open diamonds; $N = 5$, full triangle; $N = 6$, open square.

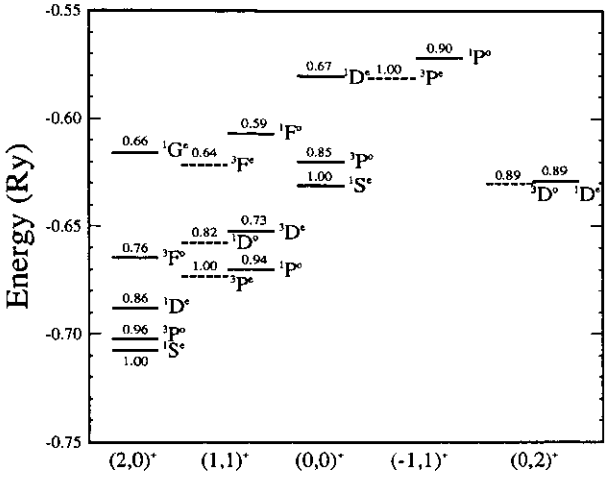

Figure 5. Fraction of the dominant T-projection for the $3l3l'$ doubly excited states of He. Each state is designated by the (K, T) quantum numbers given at the bottom of the column. For each pair of K and T, the energy of each state is ordered to show the rotor structure. The entry above each bar gives the fraction of the T-projection of that state where T is the integer designating that state. For $T \neq 0$, T-doubling is indicated for each pair.

the $T=0$ component of the ${}_N(N-1, 0)^+_N$ double Rydberg series. One can see that for each L, the fraction of the $T=0$ component is larger for the $N=4$ state than for the $N=3$ state. However, the increase with N is quite slow, see the results for $L=4$. The calculations were carried out for the He.

3.4. The purity of T-projection along the rovibrational states and T-doubling states

In figure 5 we show the energies and the fraction of the T-projection for the $3l3l'$ states of He, arranged such that each column has fixed K and T quantum numbers. The entry above each bar indicates the fraction of the T-projection of that state while the energy is indicated by the position of the bar with reference to the energy scale in the vertical axis. The decreasing fraction of this projection along the rotor series has been addressed above. Here we compare the fraction between pairs of T-doubling states.

The energies of each T-doubling pair of states are degenerate in the molecular picture if T is treated as a good quantum number. From this figure, it is clear that within each T-doubling pair, the state which has the higher percentage of the projected T component is lower in energies. In general, higher members of the rotor series have smaller fractions of the dominant T projections.

Similar comparison can be made for the $A=+1$ and $A=-1$ manifolds of the $3l4l'$ doubly excited states of He, see figure 6(a) and (b). There is no evidence that the fraction of T-projection differs significantly between intra- and intershell states.

4. Summary and discussion

In this paper we explored the limitations of the simple molecular description of doubly excited states by examining the purity of the fraction of the projection (T) of the total

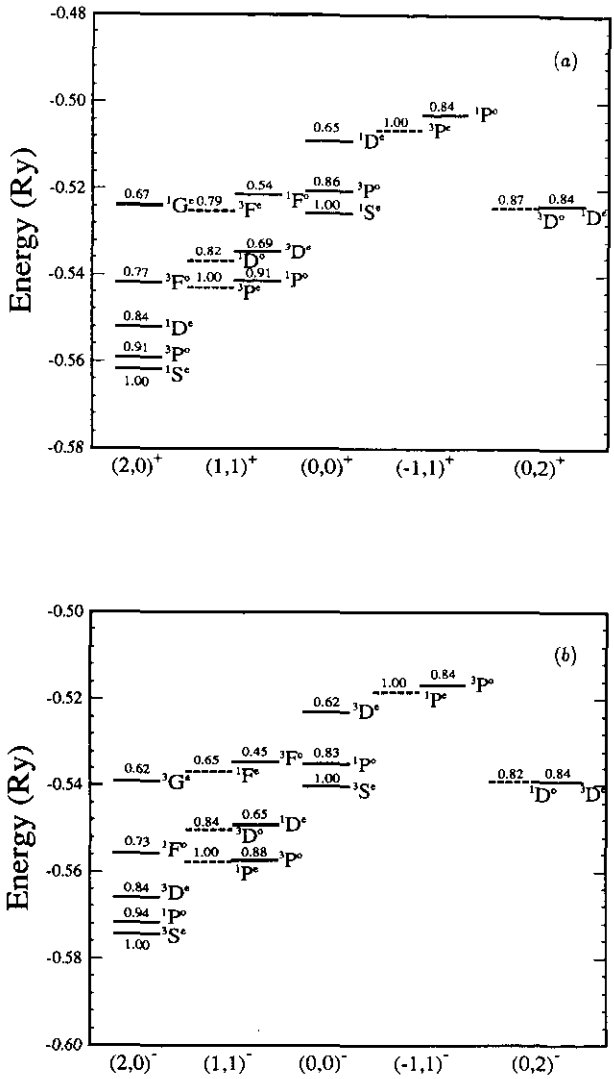

Figure 6. The same as figure 5 except for the $3l4l'$ states for (a) $A = +1$ states, (b) $A = -1$ states.

orbital angular momentum L along the interelectronic axis. A large number of doubly excited states belonging to the $3l3l'$ and $3l4l'$ doubly excited states were calculated. We showed that the small-L members of the rotor series in general have a single dominant T component, as described by quantum number T in the $(K, T)^A$ or other equivalent classification schemes. For large-L members of the rotor series, the mixture of different T components is often quite significant. These latter states are not well represented by the molecular picture.

We have also shown that the splitting between each pair of T-doubling states is due to the deviation from the simple molecular description. In other words, the small admixture of other T-component(s) is responsible for the splitting. The lower energy state within each pair always has the larger percentage of the dominant T component.

We thus conclude that deviations from the simple molecular prescriptions, such as the rotational contraction and the T-doubling, can all be related to the fact that T is not a rigorous quantum number for doubly excited states. The deviation becomes more significant in general as the angular momentum L increases.

One can also discuss doubly excited states with reference to DESB functions. The DESB functions also predict rotor-like structure for the energy levels of doubly excited states, but the origin of the rotor structure is due to the Coulomb repulsion between the electrons (Watanabe and Lin 1986) which differs from the molecular model where the rotor structure is due to the kinetic energy. The DESB functions, which contain information about the shell structure of atoms, predict directly the rotational contraction for large-L states and truncation of the rotor series. It also predicts the existence of T-doubling. All of these can be understood from the CI or the DESB functions (Dunn *et al* 1990) where high-L doubly excited states are composed of high-l orbitals from each electron. Recall that the size of the radial wavefunction decreases with increasing l for each n.

In summary, if the validity of the molecular picture is measured in terms of the purity of the T-projection along the interelectronic axis, then deviations from the molecular behaviour for each state can be assessed. We have shown that for each given state, deviations from the molecular description decrease with decreasing nuclear charge. The origin of the rotor structure for each state tends to be dominated by the potential energy term for the high-Z element and by the kinetic energy term for the low-Z element. The latter has also been analysed by Dunn *et al* (1990).

We need to point out that while deviations from a single T component can be used to assess the degree of violation of a molecular picture, the reverse is not true. A pure T-component does not imply that the system is close to a molecular description. As shown in equation (1), a Rydberg state will also have a nearly pure T-component which by no means implies that the two electrons are closely related as in a molecular description.

Acknowledgment

This work is supported in part by the US Department of Energy, Office of Basic Energy Sciences and by the US-China Cooperative Research Program.

References

Atsumi T, Ishihara T, Koyama N and Matsuzawa M 1990 *Phys. Rev.* A **42** 6391
Berry R S 1989 *Contemp. Phys.* **30** 1
Chen Z and Lin C D 1989 *Phys. Rev.* A **40** 6712
—— 1990 *Phys. Rev.* A **42** 18
Dunn M, Chen Z and Lin C D 1990 *J. Phys. B: At. Mol. Opt. Phys.* **23** 2435
Ezra G S and Berry R S 1983 *Phys. Rev.* A **28** 1974
Feagin J and Briggs J S 1987 *Phys. Rev. Lett.* **57** 984
—— 1988 *Phys. Rev.* A **37** 4599
Gou B, Chen Z and Lin C D 1991 *Phys. Rev.* A **43** 3260
Herrick D R 1983 *Adv. Chem. Phys.* **52** 1
Herrick D R and Sinanoglu O 1975 *Phys. Rev.* A **11** 97
Hunter J E III and Berry R S 1987 *Phys. Rev.* A **36** 3042
Kellman M E and Herrick D R 1980 *Phys. Rev.* A **22** 1536

Lin C D 1982 *Phys. Rev.* A **25** 76
—— 1984 *Phys. Rev.* A **29** 1019
—— 1986 *Adv. At. Mol. Phys.* **22** 77
Rost J M and Briggs J S 1988 *Z. Phys.* D **5** 339
Vollweiter A, Rost J M and Briggs J S 1991 *J. Phys. B: At. Mol. Opt. Phys.* **24** L155
Watanabe S and Lin C D 1986 *Phys. Rev.* A **34** 823
Wulfman C E 1973 *Chem. Phys. Lett.* **23** 370